AUTOPHAGY
2019, VOL. 15, NO. 9, 1523–1538
https://doi.org/10.1080/15548627.2019.1586254

Taylor & Francis
Taylor & Francis Group

RESEARCH PAPER

Autophagy-mediated *Mir6981* degradation exhibits *CDKN1B* promotion of PHLPP1 protein translation

Minggang Peng[a*], Jingjing Wang[b*], Zhongxian Tian[b*], Dongyun Zhang[a], Honglei Jin[b], Claire Liu[a], Jiawei Xu[a], Jingxia Li[a], Xiaohui Hua[a], Jiheng Xu[a], Chao Huang[a], and Chuanshu Huang[a]

[a]Department of Environmental Medicine and Urology, New York University School of Medicine, Tuxedo, NY, USA; [b]School of Laboratory Medicine and Life Science, Wenzhou Medical University, Wenzhou, Zhejiang, China

ABSTRACT

PHLPP1 (PH domain and leucine rich repeat protein phosphatase 1) is a newly identified family of Ser/Thr phosphatases that catalyzes the dephosphorylation of a conserved regulatory motif of the AGC kinases resulting in a tumor suppressive function, while CDKN1B/p27 also acts as a tumor suppressor by regulating cell cycle, senescence, apoptosis, and cell motility. Our most recent studies reveal that CDKN1B is required for PHLPP1 abundance, which contributes to the inhibition of carcinogenic arsenite-induced cell malignant transformation through inhibition of RPS6-mediated *Hif1a* translation. However, nothing is known about the mechanisms underlying the crosstalk between these 2 key tumor suppressors in intact cells. Here, for the first time to the best of our knowledge, we show that CDKN1B is able to promote PHLPP1 protein translation by attenuating the abundance of *Mir6981*, which binds directly to the 5′untranslated region (UTR) of *Phlpp1* mRNA. Further studies indicate that the attenuation of *Mir6981* expression is due to macroautophagy/autophagy-mediated degradation of *Mir6981* in an SQSTM1/p62-dependent fashion. Moreover, we have determined that *Sqstm1* is upregulated by CDKN1B at the level of transcription *via* enhancing SP1 protein stability in an HSP90-depdendent manner. Collectively, our studies prove that: 1) SQSTM1 is a CDKN1B downstream effector responsible for CDKN1B-mediated autophagy; 2) by promoting the autophagy-mediated degradation of *Mir6981*, CDKN1B exerts a positive regulatory effect on PHLPP1 translation; 3) *Mir6981* suppresses PHLPP1 translation by binding directly to its mRNA 5′-UTR, rather than classical binding to the 3′-UTR. These findings provide significant insight into understanding the crosstalk between CDKN1B and PHLPP1.

Abbreviations: ATG: autophagy related; ACTB: actin beta; BAF: bafilomycin; BECN1: beclin 1; *Cdkn1b/p27*: cyclin-dependent kinase inhibitor 1B; CHX: cycloheximide; DMEM: dulbecco's modified eagle medium; FBS: fetal bovine serum; GAPDH: glyceraldehyde −3-phosphate dehydrogenase; *Hif1a*: hypoxia inducible factor 1, alpha subunit; *Hsp90*: heat shock protein 90; JUN: Jun proto-oncogene, AP1 transcription factor subunit; MAP1LC3/LC3: microtubule-associated protein 1 light chain 3; MG132: proteasome inhibitor; *Mtor*: mechanistic target of rapamycin kinase; *Phlpp1*: PH domain and leucine rich repeat protein phosphatase 1; *Phlpp2*: PH domain and leucine rich repeat protein phosphatase 2; *Pp2c*: protein phosphatase 2 C; RPS6: ribosomal protein S6; *Sp1*: trans-acting transcription factor 1; *Sqstm1/p62*: sequestosome 1; TUBA: alpha tubulin; 3′-UTR; 3′-untranslated region; 5′-UTR: 5′-untranslated region.

ARTICLE HISTORY
Received 3 November 2017
Revised 31 January 2019
Accepted 11 February 2019

KEYWORDS
Autophagy; *Cdkn1b*; *Mir6981*; *Phlpp1*; *Sqstm1*

Introduction

The pleckstrin homology domain leucine-rich repeat protein phosphatases (PHLPPs) are novel members of the protein phosphatase 2C (PP2C) group in the family of Ser/Thr phosphatase [1]. Recent studies from various groups indicate that PHLPP functions as a tumor suppressor by regulating the signaling pathways of AKT, PKC, and JUN [2]. CDKN1B/KIP1 is also known to be a tumor suppressor by virtue of its action as a cyclin-dependent kinase inhibitor in the regulation of cell cycle, apoptosis, tumor progression, and invasion [3]. Unlike other classic tumor suppressors such as *TP53* and *RB, CDKN1B* nor *PHLPP1* are rarely mutated or deleted in human cancers [4]. The crosstalk between these 2 tumor suppressors has never been explored. Recently, our lab has shown that the N terminus of CDKN1B mediates PHLPP1 expression responsible for the inhibition of HIF1A translation following arsenite exposure [5]. Here we verify that CDKN1B can promote autophagy-mediated *Mir6981* degradation, which subsequently decreases its binding to 5′-UTR of *Phlpp1* mRNA, in turn increasing PHLPP1 translation.

miRNAs are small non-coding RNAs that play critical roles in a wide variety of biologic processes through interaction with partially complementary target sites in mRNAs [6]. Similar to other Argonaute-bound small RNAs, miRNAs also target mRNAs based on approximately 7 nt complementary base-pairing, preferentially at nucleotides 2 to 8 from the 5′ end of a mature miRNA, consequently resulting in the degradation or translational suppression of their targeted

CONTACT Chuanshu Huang Chuanshu.huang@nyumc.org Nelson Institute of Environmental Medicine, New York University School of Medicine, 57 Old Forge Road, Tuxedo, NY 10987, USA

*These authors contributed equally to this work.

mRNAs [7]. The expression level of a mature miRNA is determined by the rate of its transcription, biogenesis processing, and turnover [8]. Even though transcription regulation accounts for most of the alterations in miRNA expression, in spite of the elevation of their primary transcripts and precursors, a significant portion of mature miRNAs are downregulated [9]. The posttranscriptional regulation of miRNA is through either maturation or degradation. In our current studies, we have identified a novel mechanism of *Mir6981* alteration through autophagy by binding with the autophagy receptor SQSTM1. This *Mir6981* affects its targeted *Phlpp1* mRNA translation by binding to the 5′-untranslated region (UTR) rather than the classical 3′-UTR of *Phlpp1* mRNA.

Although it has been thought that miRNAs mainly target mRNA 3′-UTR (3′ untranslated region) and result in gene silencing *via* translational repression and/or RNA degradation [10], a recent study provides new insight into the functional roles of the 5′-UTR in mRNA repression mediated by miRNAs [11]. On the one hand, the 5′-UTR contains several regulatory elements, such as binding sites for RNA binding proteins and upstream open reading frames, which have a significant impact on the regulation of protein translation. On the other hand, the 5′-UTR has structured RNAs near the 5′ cap site, which is sufficient to block translation initiation [12]. Here, we have discovered that *Mir6981* is able to bind to the 5′-UTR of *Phlpp1* mRNA and repress PHLPP1 protein translation.

Autophagy is an evolutionarily conserved cell survival mechanism used by stressed cells to degrade the unwanted cytoplasmic proteins or organelles [13]. Autophagy is activated by metabolic stresses (such as starvation), infective pathogens and other specific substrates, as well as mediated by a specific autophagy receptor to degrade targeted protein aggregates [14]. In mammalian cells, SQSTM1 has been identified as the first autophagy receptor and acts as a scaffold for the intracellular signaling that control various cell functions [15–18]. A specific region called LIR/LRS (LC3-interacting region/LC3-recognition sequence) of mouse *Sqstm1* [19] enables the SQSTM1 targeted proteins to be recognized by the phagophore through LC3 [20]. In the current study, we reveal that CDKN1B is able to promote *Sqstm1* transcription through substantially activating SP1, and increasing SQSTM1 binding to *Mir6981*, resulting in autophagy-dependent *Mir6981* degradation, in turn attenuating *Mir6981* inhibition of PHLPP1 translation. Our results, for the first time, to the best of our knowledge, highlight the novel crosstalk between 2 tumor suppressors, CDKN1B and PHLPP1.

Results

CDKN1B specifically promoted PHLPP1 protein translation in intact cells

CDKN1B is known to be a tumor suppressor as the result of its action as a cyclin-dependent kinase inhibitor for regulating the cell cycle and growth [21]. *cdkn1b(Δ51)* corresponds to MEFs that have been derived from an embryo with a disrupted *Cdkn1b* gene, encoding amino acids 52 to 198 of the CDKN1B protein, as described in Dr. Andrew Koff's published paper [22]. The *cdkn1b*$^{-/-}$ MEFs harboring deletion of the entire coding region of mouse *Cdkn1b* were the generous gift of Dr. James Roberts [23]. *cdkn1b(Δ51)* and *Cdkn1b*$^{+/+}$ cells were first subjected to cell cycle and cell proliferation assays to validate the behavior of the cell lines. As shown in Figure S1(a), the deletion of *Cdkn1b* in *cdkn1b(Δ51)* cells increased the proportion of cells in S phase and G_2/M phase, and reduced the G_0/G_1 phase, in comparison to those in the *Cdkn1b*$^{+/+}$ cells. Consistently, cell proliferation ability in *cdkn1b(Δ51)* cells was also elevated in comparison to *Cdkn1b*$^{+/+}$cells (Figure S1(b)). We next explored the mechanisms of CDKN1B regulation of PHLPP1 by employing *Cdkn1b*$^{+/+}$ and *cdkn1b(Δ51)* cells. As expected, knockout of *Cdkn1b* almost completely abolished PHLPP1 protein expression in comparison to *Cdkn1b*$^{+/+}$ cells (Figure 1(a)), suggesting that CDKN1B positively regulates PHLPP1 protein expression. This notion was greatly supported by the data obtained from knockdown of *Cdkn1b* using *Cdkn1b* shRNA in both *Cdkn1b*$^{+/+}$ cells (Figure 1(b)) and mouse epithelial Cl41 cells (Figure 1(c)). Consistently, reintroduction of GFP-CDKN1B into *cdkn1b(Δ51)* cells rescued the PHLPP1 protein level (Figure 1(d)). Given the results strongly indicating that CDKN1B is a positive regulator for PHLPP1 expression, the *Phlpp1* mRNA levels were evaluated and compared between *Cdkn1b*$^{+/+}$ and *cdkn1b(Δ51)* cells. The results showed that *Phlpp1* mRNA levels are comparable in *Cdkn1b*$^{+/+}$ *vs. cdkn1b(Δ51)* cells (Figure 1(e)), and *Cdkn1b*$^{+/+}$(sh*Cdkn1b*) vs. *Cdkn1b*$^{+/+}$(Nonsense) cells (Figure 1(f)). These results suggest that PHLPP1 might be regulated by CDKN1B through either protein degradation or protein translation. To explore this notion, MG132 and calpain inhibitors were used to test their effects on PHLPP1 protein accumulation in both *Cdkn1b*$^{+/+}$ and *cdkn1b(Δ51)* cells. The results indicate that treatment of cells with either the calpain inhibitor or MG132 only cause PHLPP1 protein accumulation in *Cdkn1b*$^{+/+}$ cells, but not in *cdkn1b(Δ51)* cells (Figure 1(g,h)), providing a strong indication that CDKN1B promotes PHLPP1 protein expression through a protein degradation-independent mechanism.

To explore the potential effect of CDKN1B on PHLPP1 protein translation, an ^{35}S-methionine/cysteine pulse labeling assay was performed to monitor PHLPP1 new protein translation in *Cdkn1b*$^{+/+}$ and *cdkn1b(Δ51)* cells. As shown in Figure 1(i), the new PHLPP1 protein synthesizing rate in *cdkn1b(Δ51)* cells was remarkably impaired in comparison to *Cdkn1b*$^{+/+}$ cells, although total new protein syntheses (WCL) were higher in *cdkn1b(Δ51)* cells than that in *Cdkn1b*$^{+/+}$ cells. Our results reveal that CDKN1B is required for PHLPP1 protein translation.

Downregulation of the *Mir6981* is responsible for CDKN1B promotion of PHLPP1 protein translation via reduction of its binding to 5′-UTR, but not 3′UTR, of *Phlpp1* mRNA.

The 3′-UTR or 5′-UTR of mRNA are major regulatory regions that are targeted by either miRNAs or mRNA binding proteins to regulate mRNA stability or protein translation [10,12]. To evaluate the potential contribution of *Phlpp1* mRNA 3′-UTR in CDKN1B's promotion of PHLPP1 protein translation, we first constructed the *Phlpp1* 3′-UTR-luciferase reporter then stably transfected it into *Cdkn1b*$^{+/+}$ and *cdkn1b(Δ51)* cells. As shown in

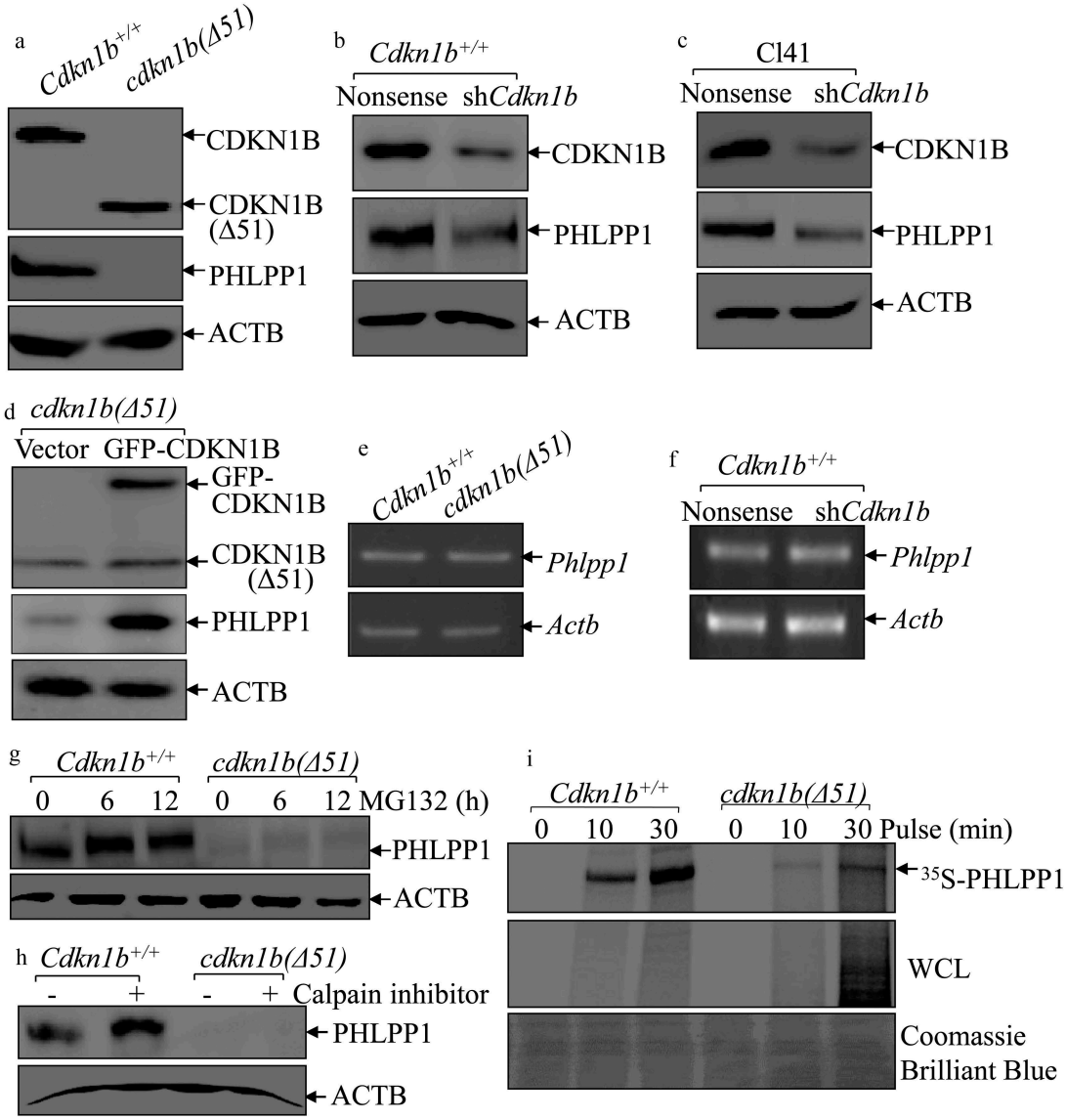

Figure 1. CDKN1B promoted PHLPP1 expression at protein translational level. (a–d) Western blots (WB) were used to determine the protein levels of PHLPP1 in *Cdkn1b*$^{+/+}$ *vs. cdkn1b(Δ51)* cells (a), *Cdkn1b*$^{+/+}$(Nonsense) *vs. Cdkn1b*$^{+/+}$(sh*Cdkn1b*) (b), Cl41(Nonsense) *vs.* Cl41(sh*Cdkn1b*) (c), and *cdkn1b(Δ51)*(Vector) *vs. cdkn1b*$^{-/-}$(Δ51)(GFP-CDKN1B) (d). ACTB was used as a protein loading control. (e,f) RT-PCR was applied to compare the *Phlpp1* mRNA levels in *Cdkn1b*$^{+/+}$ *vs. cdkn1b(Δ51)* (e) and *Cdkn1b*$^{+/+}$(Nonsense) *vs.* *Cdkn1b*$^{+/+}$(sh*Cdkn1b*) (f). *Actb* was used as an internal loading control. (g) *Cdkn1b*$^{+/+}$ and *cdkn1b(Δ51)* cells were treated with MG132 for the indicated times. The cell extracts were then subjected to western blots to determine PHLPP1 protein accumulation. ACTB was used as a protein loading control. (h) *Cdkn1b*$^{+/+}$ and *cdkn1b(Δ51)* cells were treated with Calpain inhibitor for 24 h. The cell extracts were then subjected to western blot analyses of the new PHLPP1 protein accumulation. ACTB was used as a protein loading control. (i) Newly synthesized PHLPP1 protein in *Cdkn1b*$^{+/+}$ and *cdkn1b(Δ51)* cells was monitored by ^{35}S-labeled methionine/cysteine pulse assay, as described in the section of 'Materials and Methods'. WCL, whole cell lysate. Coomassie Brilliant Blue staining was used as a protein loading control.

Figure 2(a), the *Phlpp1* 3′-UTR activity was remarkably upregulated in *cdkn1b(Δ51)* cells (Figure 2(a)), revealing that downregulation of PHLPP1 protein translation in *cdkn1b(Δ51)* cells is not attributable to 3′-UTR region of *Phlpp1* mRNA. We next tested whether 5′-UTR of *Phlpp1* mRNA was involved in CDKN1B promotion of PHLPP1 protein translation. Following construction of the *Phlpp1* mRNA 5′-UTR-luciferase reporter, it was stably transfected into *Cdkn1b*$^{+/+}$ and *cdkn1b(Δ51)* cells. As shown in Figure 2(b), the deletion of *Cdkn1b* resulted in a profound reduction of *Phlpp1* mRNA 5′-UTR activity in comparison to *Cdkn1b*$^{+/+}$ cells, suggesting that the 5′-UTR of *Phlpp1* mRNA might be implicated in CDKN1B promotion of PHLPP1 protein translation. These results indicate that CDKN1B promotes PHLPP1 protein expression with upregulation of *Phlpp1* mRNA 5′-UTR activity as well as downregulation of *Phlpp1* mRNA 3′-UTR activity. To evaluate the effect of CDKN1B on the overall activity of *Phlpp1* mRNA 3′-UTR and 5′-UTR, we constructed a *Phlpp1* mRNA luciferase reporter that contains both 5′-UTR and 3′-UTR regulatory regions. The results indicate that CDKN1B does have a positive regulatory effect on *Phlpp1* mRNA luciferase reporter under the control of both the 3′-UTR and the 5′-UTR regions (Figure 2(c)), indicating that CDKN1B positive regulation of *Phlpp1* mRNA 5′-UTR activity overcomes its negative modulation of *Phlpp1* mRNA 3′-UTR activity.

It is well-characterized that RPS6 (ribosomal protein S6) activation is essential for initiation of canonical protein translation [24]. To test whether RPS6 is involved in CDKN1B regulation of PHLPP1 protein translation, the effects of

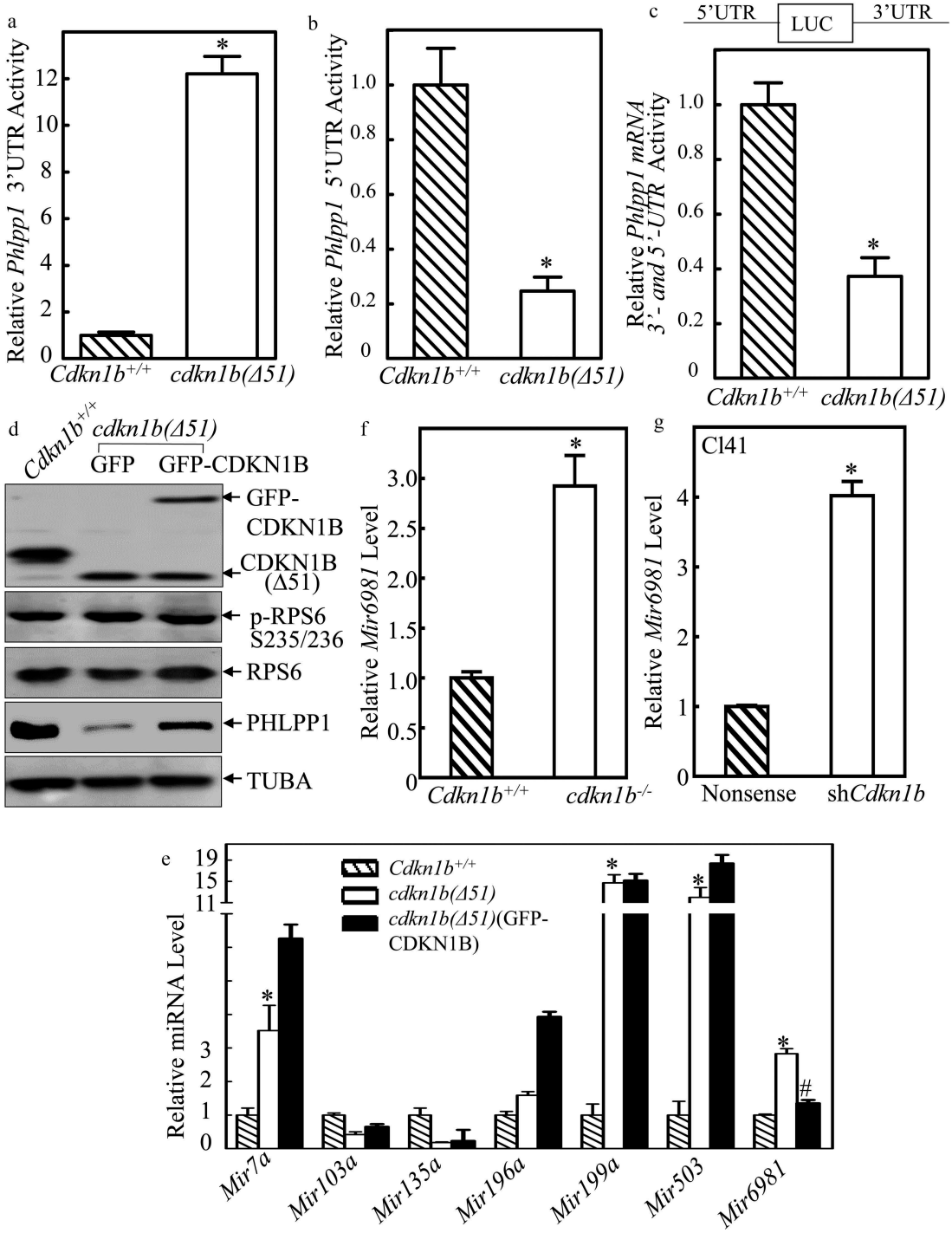

Figure 2. CDKN1B promoted *Phlpp1* mRNA 5′-UTR activity accompanied with inhibition of *Mir6981* expression. (a–c) Wild-type *Phlpp1* mRNA 3′-UTR-driven luciferase reporters(a), 5′-UTR-driven luciferase reporters (b), The luciferase reporter containing both the 5′-UTR and 3′-UTR regulatory regions (c), were cotransfected with pRL-TK into *Cdkn1b*$^{+/+}$ and *cdkn1b*(Δ51) cells, respectively. Twenty-four h post transfection, the transfectants were extracted for evaluation of the luciferase activity. TK was used as an internal control. The results were presented as *Phlpp1* 3′-UTR activity (a), 5′-UTR activity (b), or *Phlpp1* mRNA 3′ and 5′-UTR activity (c) relative to *Cdkn1b*$^{+/+}$ cells. Each bar indicates a mean±SD of triplicates. The symbol (*) indicates a significant difference in comparison to *Cdkn1b*$^{+/+}$ cells ($P < 0.05$). (d) Cell extracts from *Cdkn1b*$^{+/+}$, *cdkn1b(Δ51)*(GFP), and *cdkn1b(Δ51)*(GFP-CDKN1B) cells were subjected to western blot analysis for protein expression of CDKN1B, P-RPS6, RPS6, and PHLPP1. TUBA was used as a protein loading control. (e) For the cells indicated, the expression levels of *Mir7a, Mir103a, Mir135a, Mir196a, Mir199a, Mir503*, and *Mir6981* were evaluated by real-time PCR. The results were normalized to *Rnu6*. The symbol (*) indicates a significant increase in comparison to *Cdkn1b*$^{+/+}$ cells, while the symbol '#' indicates significant inhibition in comparison to *cdkn1b(Δ51)* cells ($P < 0.05$). (f,g) The expression levels of *Mir6981* were evaluated by real-time PCR in *Cdkn1b*$^{+/+}$ *vs. cdkn1b*$^{-/-}$ cells (f), and Cl41(Nonsense) *vs.* Cl41(sh*Cdkn1b*) cells (g). The results were normalized to *Rnu6*. Each bar indicates a mean±SD of triplicates. The symbol (*) indicates a significant difference in comparison to *Cdkn1b*$^{+/+}$ cells or Cl41(Nonsense) cells ($P < 0.05$).

CDKN1B on activation of RPS6 were evaluated in *Cdkn1b*$^{+/+}$, *cdkn1b(Δ51)*(GFP) and *cdkn1b(Δ51)*(GFP-CDKN1B) cells. As shown in Figure 2(d), there was no observable alteration of RPS6 phosphorylation among the 3 cells, whereas *Cdkn1b* deletion resulted in a dramatic inhibition of PHLPP1 protein abundance. Moreover, the PHLPP1 protein defect can be

rescued by constitutively expressing GFP-CDKN1B into *cdkn1b(Δ51)* cells. These results suggest that RPS6 activation might not be involved in CDKN1B promotion of PHLPP1 protein translation.

Therefore, we next sought to determine whether miRNA could be a CDKN1B downstream effector for its regulation of *Phlpp1* mRNA 5′-UTR activity. The results obtained from the bioinformatics analysis for the putative miRNA binding sites indicate that 5′-UTR region of *Phlpp1* mRNA contains the multiple miRNA binding sites, including *Mir7a, Mir103a, Mir135a, Mir196a, Mir199a, Mir503a*, and *Mir6981* (Table 1). To define the specific miRNA that might be involved in CDKN1B promotion of *Phlpp1* mRNA 5′-UTR activity, the listed miRNA expression levels were determined in *Cdkn1b*$^{+/+}$, *cdkn1b(Δ51)*(GFP), and *cdkn1b(Δ51)* (GFP-CDKN1B) cells which have recovered the CDKN1B expression. As shown in Figure 2(e), the expression levels of *Mir7a, Mir199a, Mir503*, and *Mir6981*, but not *Mir103a, Mir135a*, and *Mir196a*, were significantly elevated in *cdkn1b(Δ51)* cells in comparison to *Cdkn1b*$^{+/+}$ cells. By ectopic expression of GFP-CDKN1B in *cdkn1b(Δ51)* cells, we discovered that only expression of *Mir6981* could be inhibited by overexpression of GFP-CDKN1B in *cdkn1b(Δ51)* cells (Figure 2(e)), revealing that the inhibition of *Mir6981* might contribute to CDKN1B promotion of PHLPP1 protein translation by targeting its mRNA 5′-UTR region. This notion was further supported by the results obtained from utilization of *Cdkn1b*$^{+/+}$ and *cdkn1b*$^{-/-}$ cells (Figure 2(f)) and knockdown of *Cdkn1b* in Cl41 cells (Figure 2(g)).

To define the role of *Mir6981* in attenuating PHLPP1 translation in both *Cdkn1b*$^{+/+}$ and *cdkn1b(Δ51)* cells, we stably transfected *Mir6981* into *Cdkn1b*$^{+/+}$ cells and *Mir6981* inhibitor (Inh) into *cdkn1b(Δ51)* cells. The results indicated that the *Mir6981* transfectant did exhibit overexpression, while *Mir6981* Inh inhibited *Mir6981* expression in comparison to their scrambled control vector transfectants (Figure 3(a)). Consistently, overexpression of *Mir6981* in *Cdkn1b*$^{+/+}$ cells profoundly inhibited *Phlpp1* mRNA 5′-UTR activity and attenuated PHLPP1 protein expression (Figure 3(b,c)), whereas ectopic expression of *Mir6981* inhibitor significantly increased *Phlpp1* mRNA 5′-UTR activity, along with elevating PHLPP1 protein expression in *cdkn1b(Δ51)* cells (Figure 3(b,d)). Moreover, inhibition of *Phlpp1* mRNA 5′-UTR activity by *Mir6981* in *Cdkn1b*$^{+/+}$ cells was not observed in the *Cdkn1b*$^{+/+}$ cells stably transfected with the *Mir6981* binding site point-mutated *Phlpp1* mRNA 5′-UTR-luciferase reporter in comparison to that in *Cdkn1b*$^{+/+}$ cells stably transfected with wild-type *Phlpp1* mRNA 5′-UTR-luciferase reporter (WT) (Figure 3(e,f)). Collectively, our results verify that upregulated *Mir6981* in *cdkn1b(Δ51)* cells is able to inhibit PHLPP1 protein translation by directly targeting its binding site in *Phlpp1* mRNA 5′UTR region, rather than targeting *Phlpp1* mRNA 3′-UTR region.

Table 1. Sequence alignments of potential miRNAs with the *Phlpp1* 5′UTR.

Phlpp1-5′UTR: 5′…(44)CGCCGCCGCCGCCGCCGUCUCCCA (67)…	
	⏐⏐⏐⏐⏐⏐⏐
mmu-*Mir7a*: 3′ …UGUUGUUUUAGUGAUCAGAAGGU	
Phlpp1-5′UTR: 5′ …(75)CUCACCUCCUCCUCCUAUGCUGC (97)…	
	⏐⏐⏐⏐⏐⏐⏐
mmu-*Mir103a*: 3′ AGUAUCGGGACAUGUUACGACGA	
Phlpp1-5′UTR: 5′ …..(3)GAGCGGCCGCGCCGAACGCCAU (24)…	
	⏐⏐⏐⏐⏐⏐⏐
mmu-*Mir135a*: 3′ …..AGUGUAUCCUUAUUUUUCGGUAU	
Phlpp1-5′UTR: 5′ …(79)CCUCCUCCUCCUCCACUACCU (99)…	
	⏐⏐⏐⏐⏐⏐⏐
mmu-*Mir196a*: 3′ ..GGGUUGUUGUACUUUGAUGGAU	
Phlpp1-5′UTR: 5′…(88) CCUCCGCUGCCUCCGGCACUGGG (110)…	
	⏐⏐⏐⏐⏐⏐⏐
mmu-*Mir199a*: 3′ CUUGUCCAUCAGACUUGUGACCC	
Phlpp1-5′UTR: 5′ ….(111)GGAGCGACGUGAAGCCCTGCUA (132)…	
	⏐⏐⏐⏐⏐⏐⏐
mmu-*Mir503*: 3′ ….GACGUCUUGACAAGGGCGACGAU	
Phlpp1-5′UTR: 5′….(56) CGCCGUCUCCCACCUUCGCCUCAC (79)…	
	⏐⏐⏐⏐⏐⏐⏐
mmu-*Mir6981*: 3′ CGGAAGUCGGAGAAGGAAGAGGAGUG	

CDKN1B promoted *Mir6981* degradation through upregulation of Sqstm1-mediated autophagy

The miRNA can be transcribed either along with its host gene under the control of its host gene promoter or it can be transcribed under control of its own promoter [9]. Using the NCBI gene database, *Arap3* (ArfGAP with RhoGAP domain, ankyrin repeat and PH domain 3) was identified as the host gene for *Mir6981*, as shown in Figure 4(a). To elucidate the mechanisms of CDKN1B modulation of *Mir6981* expression, *Arap3* mRNA expression was determined in *Cdkn1b*$^{+/+}$ and *cdkn1b(Δ51)* cells. The result indicate that *Arap3* mRNA levels in *cdkn1b(Δ51)* cells and *cdkn1b*$^{-/-}$ cells were significantly attenuated in comparison to *Cdkn1b*$^{+/+}$ cells (Figure 4(b,c)). However, this is inconsistent with the elevation of *Mir6981* expression in *cdkn1b(Δ51)* cells; thereby excluding the possibility that CDKN1B regulates *Mir6981* transcription. This notion is further supported by the results showing that pre-*Mir6981* was significantly impaired in both *cdkn1b(Δ51)* and *cdkn1b*$^{-/-}$ cells, in comparison to those observed in their corresponding *Cdkn1b*$^{+/+}$ cells (Figure. 4(d,e)). Thus, we next tested the potential effect of CDKN1B on *Mir6981* degradation. ACTD was used to block new miRNA transcription to evaluate *Mir6981* degradation rates in both *Cdkn1b*$^{+/+}$ and *cdkn1b(Δ51)* cells. The results indicate that *Mir6981* degradation in *cdkn1b(Δ51)* cells is retarded in comparison to *Cdkn1b*$^{+/+}$ cells (Figure 4(f)), providing significant evidence that CDKN1B promotes *Mir6981* degradation.

To the best of our knowledge, there have been very few reports about the mechanisms underlying the regulation of miRNA degradation by autophagy. To explore the potential involvement of autophagy in the degradation of *Mir6981*, we employed bafilomycin (BAF), an autophagy inhibitor. As shown in Figure 4(g,h), the treatment of cells with BAF led to a dramatic inhibition of autophagy, together with a remarkable elevation of *Mir6981* expression in *Cdkn1b*$^{+/+}$ cells, suggesting that autophagic response is involved in the regulation of *Mir6981* stability. Consistently, *cdkn1b(Δ51)* cells showed a reduction of autophagy (Figure 4(h)) and an increase in *Mir6981* levels in the absence of BAF treatment (Figure 4(g)). It was interesting to note that BAF treatment showed less effect on elevation of *Mir6981* in *cdkn1b*$^{-/-}$*(Δ51)* cells in comparison to *Cdkn1b*$^{+/+}$ cells (Figure 4(g)). Possible reason that BAF shows less effect on autophagic activity in *cdkn1b(Δ51)* cells is because there already is a low basal level of autophagy in *cdkn1b(Δ51)* cells. Our results reveal that

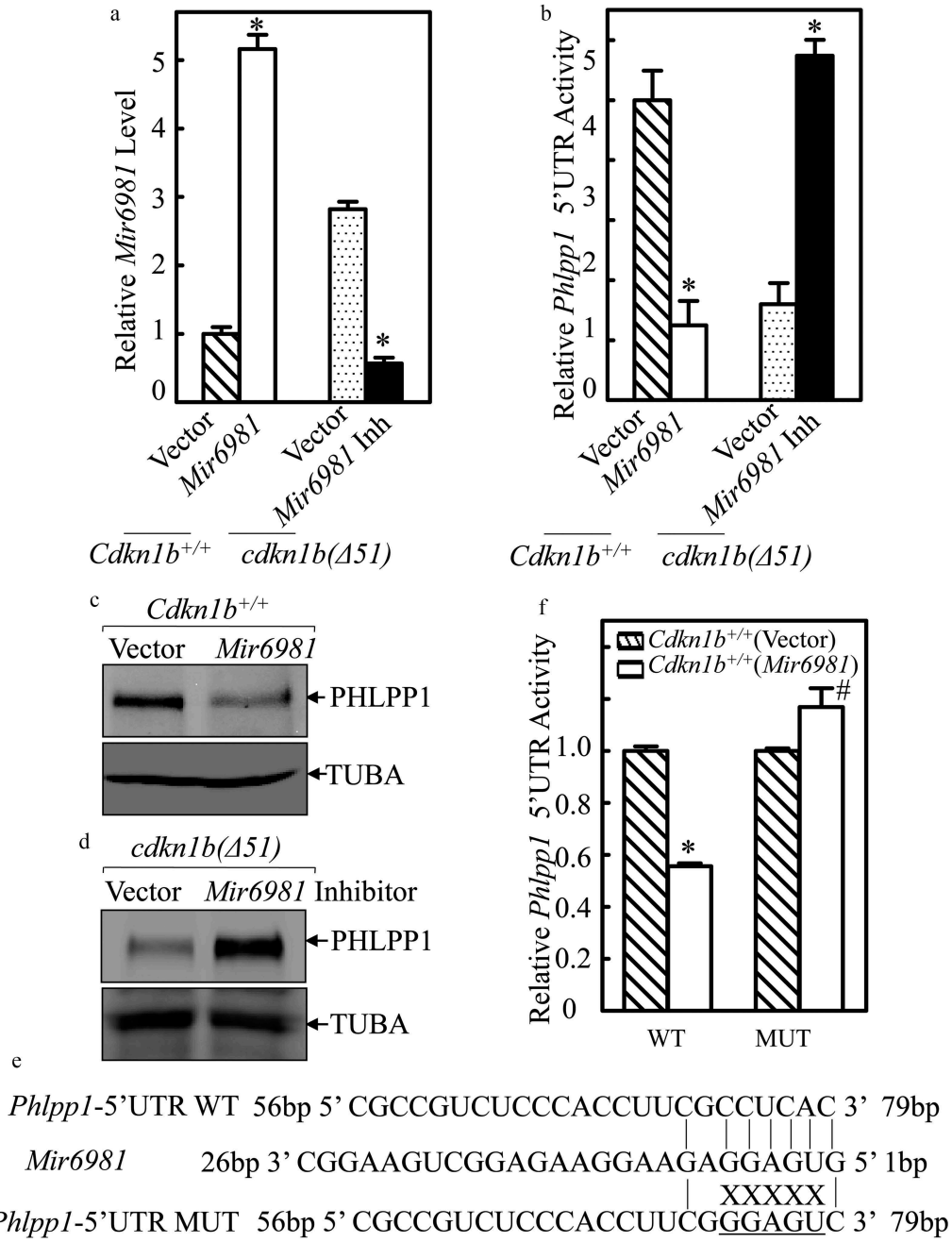

Figure 3. The *Mir6981* binding site in 5′-UTR of *Phlpp1* mRNA was required for *Mir6981* inhibition of *Phlpp1* 5′-UTR activity and protein expression. (a) Real-time PCR was employed to identify the expression levels of *Mir6981* in *Cdkn1b*$^{+/+}$ cells with overexpressed *Mir6981* and *cdkn1b(Δ51)* cells stably transfected with *Mir6981* inhibitor. (b) Wild-type *Phlpp1* mRNA 5′-UTR-driven luciferase reporters were cotransfected with pRL-TK into *Cdkn1b*$^{+/+}$ *vs.* *Cdkn1b*$^{+/+}$(*Mir6981*) cells and *cdkn1b(Δ51) vs. cdkn1b(Δ51)* (*Mir6981* inhibitor) cells, respectively. Twenty-four h post transfection, the transfectants were extracted to evaluate the luciferase activity. TK was used as an internal control. The results were presented as *Phlpp1* 5′-UTR activity relative to scrambled control vector transfectants. The symbol (*) indicates a significant difference ($P < 0.05$). (c,d) The protein levels of PHLPP1 in *Cdkn1b*$^{+/+}$ cells with overexpressed *Mir6981* (c) and *cdkn1b(Δ51)* cells stably transfected with *Mir6981* inhibitor (d) were determined by western blots with TUBA as a loading control. (e) The illustration of *Mir6981* binding to the *Phlpp1* mRNA 5′-UTR region and *Mir6981* binding site mutation. (f) Wild type and mutant of *Phlpp1* mRNA 5′-UTR-driven luciferase reporters were co-transfected with pRL-TK into *Cdkn1b*$^{+/+}$ and *Cdkn1b*$^{+/+}$(*Mir6981*) cells. Twenty-four h post transfection, the transfectants were extracted to determine the luciferase activity. TK was used as an internal control. The results are presented as *Phlpp1* 5′-UTR activity relative to *Cdkn1b*$^{+/+}$(vector) cells. The symbol (*) indicates a significant inhibition in comparison to *Cdkn1b*$^{+/+}$(vector) cells ($P < 0.05$).

CDKN1B is critical for *Mir6981* degradation through an autophagy-dependent mechanism. We next evaluated whether CDKN1B expression participated in autophagic response in intact cells. The results indicate that although *Cdkn1b* deletion exhibited a reduction of cell autophagy along with inhibition of protein expression of ATG3, ATG12–ATG5, ATG7, BECN1, and SQSTM1, ectopic restoration of GFP-CDKN1B in *cdkn1b(Δ51)* cells resulted in an increase in cell autophagy with a marked induction of only SQSTM1 and BECN1 (Figures 4(h,i) and S2), indicating that CDKN1B expression is positively related to expression of SQSTM1 and BECN1, which might contribute to the autophagic regulation of

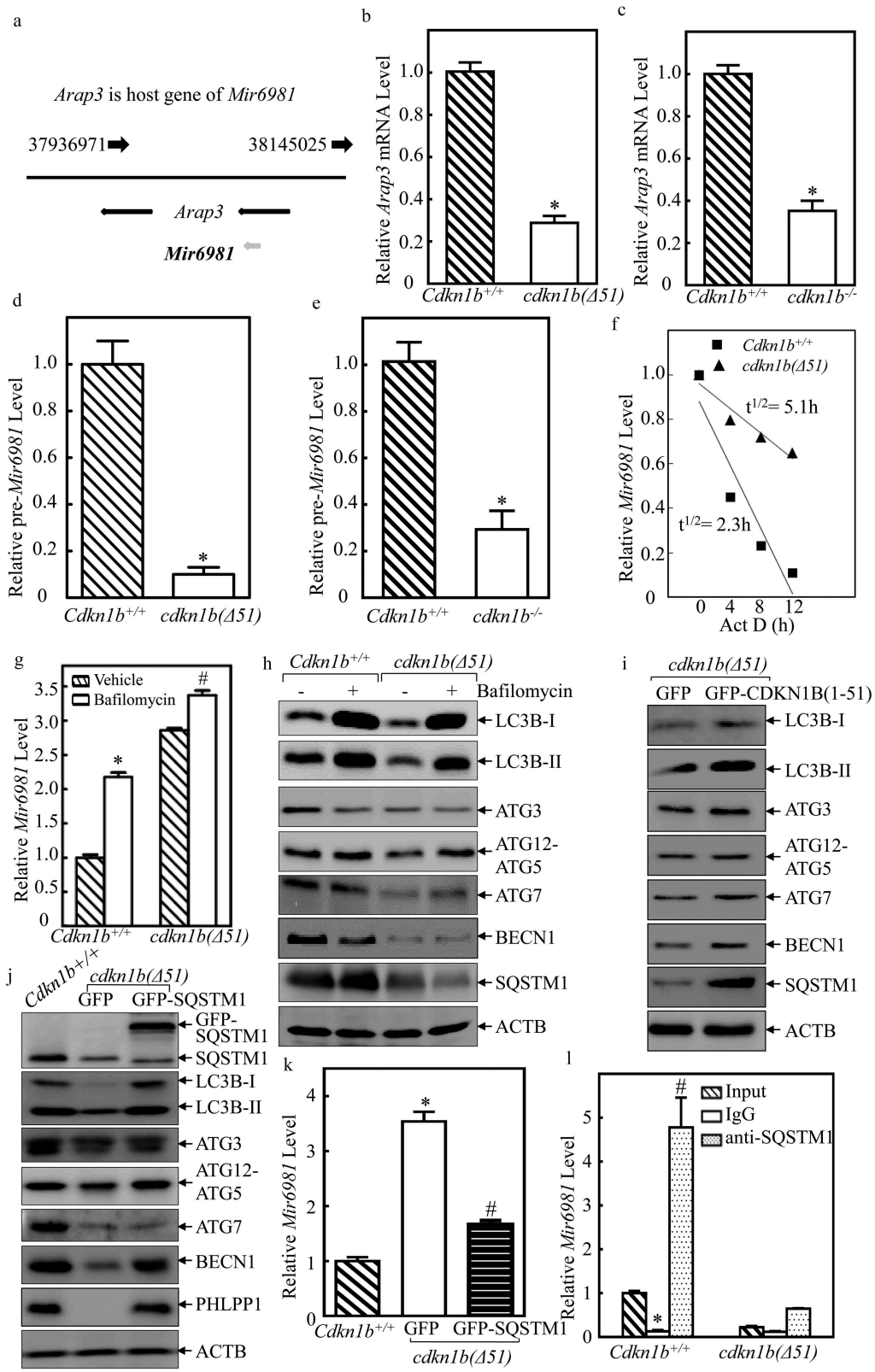

Figure 4. *Mir6981* was degraded through a CDKN1B-mediated autophagic mechanism in SQSTM1-dependent manner. (a) The illustration of *Arap3* as the host gene of *Mir6981*. (b,c) RT-PCR was employed to compare the mRNA levels of *Arap3* in *Cdkn1b*$^{+/+}$ vs. *cdkn1b(Δ51)* cells (b) and *Cdkn1b*$^{+/+}$ vs. *cdkn1b*$^{-/-}$ cells (c), respectively. *Actb* was used as a loading control. (d,e) The expression levels pre-*Mir6981* were evaluated by real-time PCR in *Cdkn1b*$^{+/+}$ vs. *cdkn1b(Δ51)* cells (d) and *Cdkn1b*$^{+/+}$ vs. *cdkn1b*$^{-/-}$ cells (e), respectively. The symbol (*) indicates significant inhibition ($P < 0.05$). (f) *Mir6981* stabilities were determined by real-time PCR in the presence of actinomycin D in *Cdkn1b*$^{+/+}$ and *cdkn1b(Δ51)* cells. (g) Real-time PCR was employed to evaluate the expression level of *Mir6981* in *Cdkn1b*$^{+/+}$ cells and *cdkn1b(Δ51)* cells in the presence or absence of BAF treatment. The symbol (*) indicates a significant increase in comparison to the vehicle control ($P < 0.05$). (h) Western blots were employed to evaluate the indicated protein expression in *Cdkn1b*$^{+/+}$ cells and *cdkn1b(Δ51)* cells in the presence or absence of BAF treatment. (i,j) Western blots were employed to determine the indicated protein expressions in *cdkn1b (Δ51)* (Vector) *vs. cdkn1b(Δ51)*(GFP-CDKN1B) cells (i) or in *Cdkn1b*$^{+/+}$ *vs. cdkn1b(Δ51)*(GFP) cells *vs. cdkn1b*(Δ51)(GFP-SQSTM1) cells (j). ACTB was used as a protein loading control. (k) The expression levels of *Mir6981* in *Cdkn1b*$^{+/+}$, *cdkn1b(Δ51)*(GFP) cells, and *cdkn1b(Δ51)*(GFP-SQSTM1) cells were determined by real-time PCR. (l) An RNA-IP assay was employed to evaluate the potential interaction between SQSTM1 protein and *Mir6981* in *Cdkn1b*$^{+/+}$ cells and *cdkn1b(Δ51)* cells. Real-time PCR was employed to determine *Mir6981* levels in the immuno-complex affinity-isolation by anti-SQSTM1 antibody.

Mir6981 degradation. To test the potential contribution of SQSTM1 to CDKN1B-regulated *Mir6981*, GFP-SQSTM1 was stably transfected into *cdkn1b(Δ51)* cells. The results show that overexpression of SQSTM1 led to a profound increase in LC3B-II level and BECN1 expression, as well as PHLPP1 expression (Figure 4(j)), revealing that SQSTM1 is an upstream regulator for induction of BECN1 and autophagy. Our next step was to evaluate the possible regulatory effect of SQSTM1 on *Mir6981* degradation in *cdkn1b(Δ51)* (GFP-SQSTM1) cells in comparison to *cdkn1b(Δ51)* (GFP) cells. As exhibited in Figure 4(k), ectopic expression of GFP-SQSTM1 in *cdkn1b(Δ51)* showed that there is a significant inhibition of *Mir6981* expression. To assess the role of CDKN1B-regulated BECN1 and ATG7 in CDKN1B-mediated autophagy and PHLPP1 protein expression, we overexpressed GFP-ATG7 and GFP-BECN1, into *cdkn1b (Δ51)* cells. The results show that overexpression of ATG7 does not have any observable regulation of autophagy and PHLPP1 levels, whereas GFP-BECN1 overexpression has only a slight effect (Figure S3(a,b)). Moreover, the results obtained from RNA-IP assay indicate that SQSTM1 has a strong binding activity to *Mir6981* in the immune-complex that was pulled down using anti-SQSTM1 antibodies (Figure 4(l)).

SP1 was a downstream transcription factor responsible for CDKN1B-regulated *Sqstm1* transcription

To elucidate the mechanism of CDKN1B's promotion of SQSTM1, *Sqstm1* mRNA was first analyzed in $Cdkn1b^{+/+}$ and *cdkn1b(Δ51)* cells. As shown in Figure 5(a), *Sqstm1* mRNA was attenuated in *cdkn1b(Δ51)* cells. To determine whether CDKN1B modulates *Sqstm1* at transcription level, the full length of the *Sqstm1* promoter-driven luciferase reporters together with 3 deletions, as shown in Figure 5(b), were constructed and transfected into $Cdkn1b^{+/+}$ cells and *cdkn1b(Δ51)* cells, respectively. The deletion of the *Sqstm1* promoter region was analyzed for its potential transcription factor binding sites (listed in Figure 5(b)). As observed in Figure 5(c), both the full length and 3 deletions of *Sqstm1* promoter-driven luciferase reporter showed significantly similar patterns of inhibition of promoter transcription activities in *cdkn1b(Δ51)* cells in comparison to the patterns that were seen in $Cdkn1b^{+/+}$ cells. Based on this evidence, we anticipated that the transcription factor binding site responsible for CDKN1B promotion of *Sqstm1* transcription might be in the −935 bp reporter. Our next step was to evaluate the effect of CDKN1B on the expression of the transcription factors that might potentially bind to this −935 bp region. We found that expression of E2F1, JUNB, p-JUN, JUN, and SP1 were impaired in *cdkn1b(Δ51)* cells, while ELK1 was comparable between the 2 cells (Figures 5(d) and S4(a)). Given that JUNB has been most commonly reported to inhibit its regulated gene transcription [25], JUN and SP1 were first analyzed for their potential effects on SQSTM1 expression. As shown in Figure 5(e,f) and S4(b,c), inhibition of JUN activation by ectopic expression of a dominant negative mutant of JUN (TAM67) slightly increased SQSTM1 expression, while knockdown of *Sp1* led to a dramatic decrease in SQSTM1 expression in $Cdkn1b^{+/+}$ cells, indicating that SP1, but not JUN, has a role in SQSTM1 expression in $Cdkn1b^{+/+}$ cells. This notion is supported by the results showing that ectopic expression of SP1 increased SQSTM1 protein levels in *cdkn1b(Δ51)* cells (Figures 5(g) and S4(d)). Moreover, the results obtained from *Sqstm1* promoter-driven luciferase reporter assay reveal that CDKN1B expression inhibits *Sqstm1* promoter-driven luciferase reporter activity, whereas this inhibition by CDKN1B was completely abolished if the SP1 binding site in *Sqstm1* promoter-driven luciferase reporter was point mutated (Figure 5(h,i)). In addition, the results from the CHIP assay reveal that SP1 can directly bind to the *Sqstm1* promoter at the putative *Sp1* binding site at −47 bp (Figure 5(j)). Taken together, these results provide strong evidence that SP1 is specifically regulated by CDKN1B, which in turn, activates *Sqstm1* transcription and increases its protein expression.

Upregulated HSP90 mediated CDKN1B stabilization of SP1 protein

To explore the mechanism underlying SP1 regulation by CDKN1B, we evaluated *Sp1* mRNA levels in $Cdkn1b^{+/+}$ and *cdkn1b(Δ51)* cells and found that *Sp1* mRNA expression was comparable between these 2 cells (Figure 6(a)), demonstrating that SP1 is regulated by CDKN1B, either through protein stability or protein translation. To test this, CHX was utilized to inhibit new protein synthesis to evaluate SP1 protein degradation rates between $Cdkn1b^{+/+}$ and *cdkn1b(Δ51)* cells. As shown in Figure 6(b), SP1 degradation in *cdkn1b(Δ51)* cells was higher than that in $Cdkn1b^{+/+}$ cells, indicating that CDKN1B might have a function in the stabilization of the SP1 protein. Because HSP90 can bind and stabilize SP1 protein [26], we analyzed HSP90 levels in $Cdkn1b^{+/+}$ and *cdkn1b(Δ51)* cells and found that the protein abundance of HSP90 was significantly attenuated in *cdkn1b(Δ51)* cells in comparison to the amount in $Cdkn1b^{+/+}$ cells (Figure 6(c)). To further evaluate the contribution of HSP90 to the maintenance of SP1 stability, we introduced HSP90 and GFP-CDKN1B ectopic-expressing constructs into *cdkn1b(Δ51)* cells. While GFP-CDKN1B construct was overexpressed in *cdkn1b(Δ51)* to observe its effect on its downstream molecules and to determine whether GFP-CDKN1B restores HSP90 abundance. As shown in Figure 6(d), overexpression of GFP-CDKN1B in *cdkn1b(Δ51)* cells restores HSP90 expression, while either ectopic expression of HSP90 or GFP-CDKN1B rescued protein expression of SP1, SQSTM1, LC3B, and PHLPP1 protein (Figure 6(d)), revealing that CDKN1B plays an essential role in maintaining these protein expressions. This is supported by the results obtained from the $cdkn1b^{-/-}$ and Cl41 (sh*Cdkn1b*) cells (Figure 6(e,f)). It is noted that although GFP-CDKN1B protein expression in *cdkn1b(Δ51)*(GFP-CDKN1B) cells is relatively lower than that in $Cdkn1b^{+/+}$ cells. However, this GFP-CDKN1B seems to be sufficient to rescue the levels of HSP90, SP1, SQSTM1, LC3B, and PHLPP1 proteins to levels similar to those observed in $Cdkn1b^{+/+}$ cells (Figure 6(d)). It could be possible that the introduced GFP-CDKN1B is able to bring up the CDKN1B level in *cdkn1b(Δ51)* cells to the threshold level that is necessary to activate the HSP90-SP1-SQSTM1 axis. Consistently, compared to its vector control transfectant, *cdkn1b(Δ51)*(Vector), SP1 protein was more stable in *cdkn1b(Δ51)* (HSP90) cells with overexpressed HSP90 in *cdkn1b(Δ51)* cells (Figure 6(g)), suggesting that the increased SP1 protein degradation in *Cdkn1b* knockout

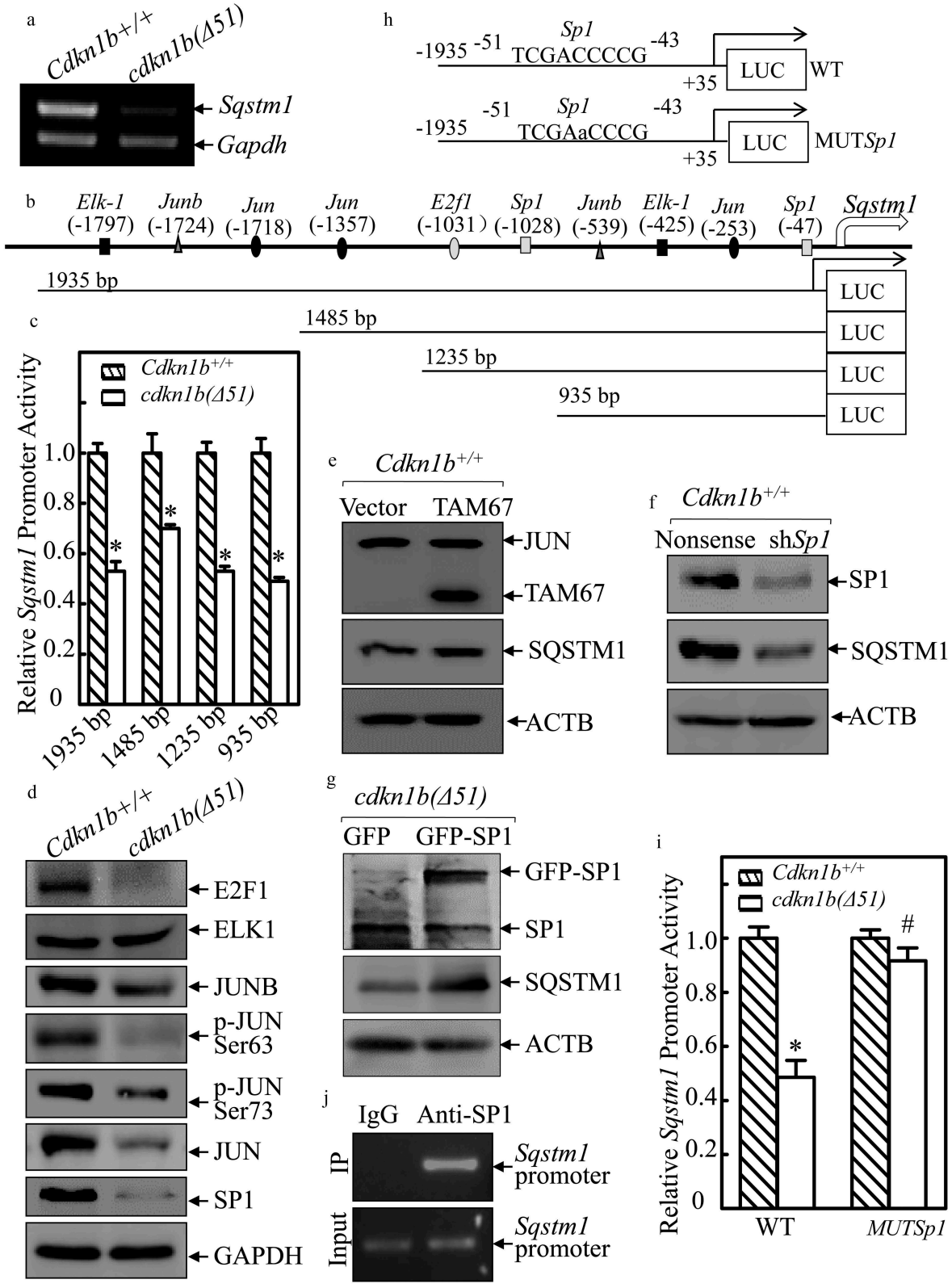

Figure 5. CDKN1B promoted *Sqstm1* mRNA transcription specifically by elevating SP1 expression. (a) RT-PCR was applied to evaluate *Sqstm1* mRNA levels in *Cdkn1b*$^{+/+}$ and *cdkn1b(Δ51)* cells. (b) The various deletions of mouse *Sqstm1* promoter-driven luciferase reporters were constructed and the putative transcription factor binding sites were analyzed using the TRANSFAC 8.3 engine online. (c) Various deletions of mouse *Sqstm1* promoter luciferase reporters were cotransfected together with pRL-TK into *Cdkn1b*$^{+/+}$ and *cdkn1b(Δ51)* cells. Twenty-four h post transfection, the transfectants were extracted to evaluate the luciferase activity. TK was used as an internal control. The results are presented as *Sqstm1* promoter activity in *cdkn1b(Δ51)* cells relative to *Cdkn1b*$^{+/+}$ cells. Each bar indicates a mean ± SD from 3 independent experiments. The symbol (*) indicates a significant reduction ($P < 0.05$). (d–g) The cell extracts from the indicated cells and their transfectants were subjected to western blots to evaluate protein expression using specific antibodies. Either GAPDH or ACTB were used as protein loading controls. (h) The diagram of the WT-*Sqstm1* promoter-driven luciferase reporter and its mutation at the SP1 binding site at −47 bp. (i) Both WT- and the mutated forms of the *Sqstm1* promoter luciferase reporters shown in Figure 5H were transiently cotransfected with pRL-TK into *Cdkn1b*$^{+/+}$ and *cdkn1b(Δ51)* cells. Twenty-four h post-transfection, the transfectants were extracted to evaluate the luciferase activity. TK was used as an internal control. The results are presented as *Sqstm1* promoter activity in *cdkn1b(Δ51)* cells relative to *Cdkn1b*$^{+/+}$ cells. The symbol (*) indicates a significant decrease in comparison to *Cdkn1b*$^{+/+}$ cells ($P < 0.05$). (j) ChIP assay was employed to evaluate SP1 binding to the *Sqstm1* promoter region using anti-SP1 antibody.

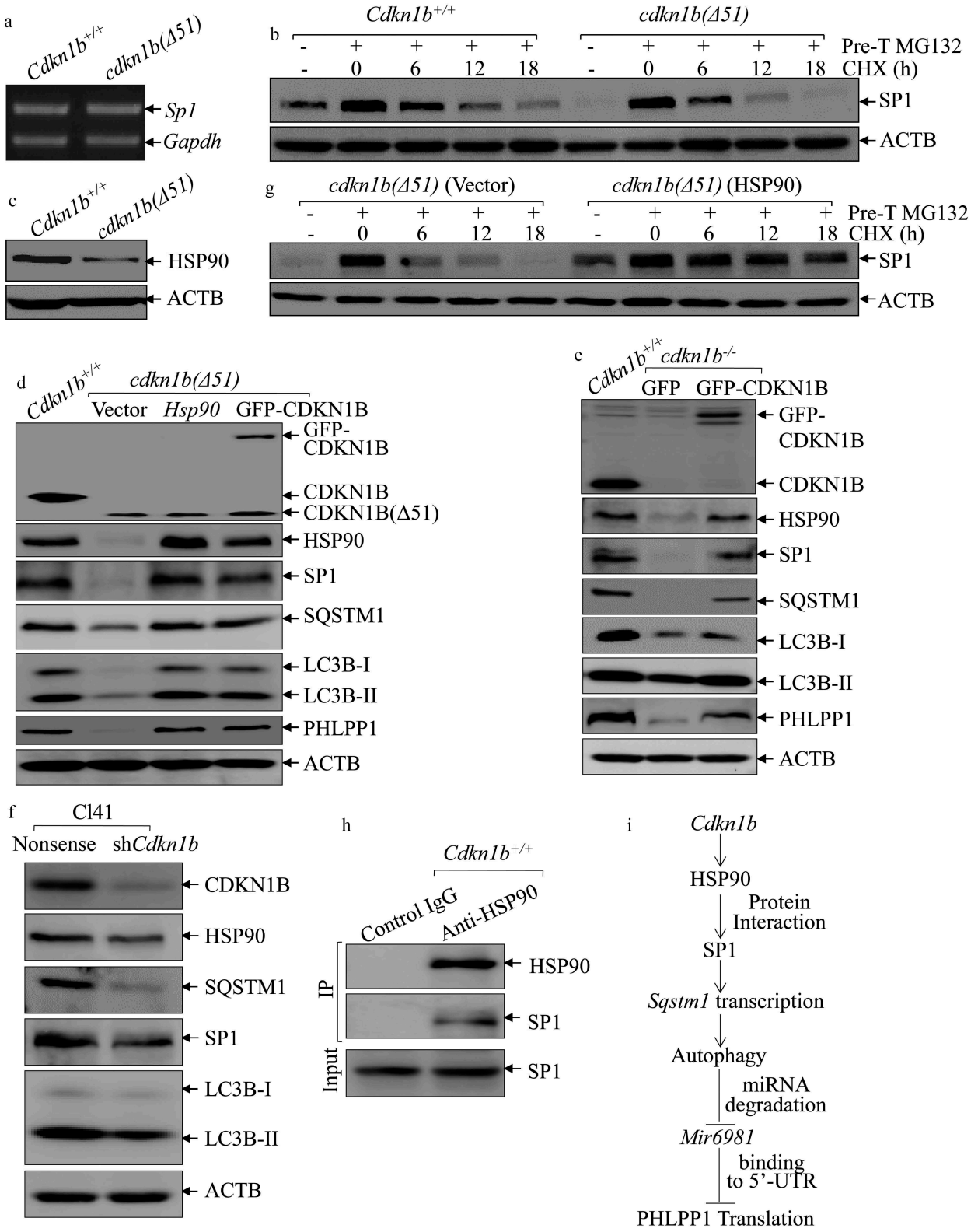

Figure 6. HSP90 acted as a CDKN1B downstream effector to stabilize the SP1 protein. (a) RT-PCR was employed to compare *Sp1* RNA levels between *Cdkn1b*$^{+/+}$ and *cdkn1b(Δ51)* cells. (b) *Cdkn1b*$^{+/+}$ and *cdkn1b(Δ51)* cells were pretreated with MG132 for 12 h, and the cells were then incubated with CHX for the indicated times. The cell extracts were then subjected to western blots to analyze SP1 protein degradation rates. ACTB was used as a protein loading control. (c) The protein level of HSP90 in *Cdkn1b*$^{+/+}$ *vs. cdkn1b(Δ51)* cells was determined by western blots and ACTB was used as a protein loading control. (d) Western blots were employed to compare protein expression between *Cdkn1b*$^{+/+}$, *cdkn1b(Δ51)*(Vector), *cdkn1b(Δ51)*(HSP90) and *cdkn1b(Δ51)*(GFP-CDKN1B) cells, as indicated. ACTB was used as a protein loading control. (e,f) The cell extracts from the indicated cells and their transfectants were subjected to western blots to evaluate protein expression using specific antibodies. ACTB were used as protein loading controls. (g) *cdkn1b(Δ51)*(Vector) and *cdkn1b(Δ51)*(HSP90) cells were treated with MG132 for 12 h and the cells were then incubated with CHX for the indicated times. The cell extracts were subjected to western blots to analyze SP1 protein degradation rates. ACTB was used as a protein loading control. (h) An immunoprecipitation assay was employed to determine SP1 protein interaction with HSP90 using an anti-HSP90 antibody. (i) Schematic model for CDKN1B promotion of *Mir6981* degradation and PHLPP1 protein translation.

cells could be stabilized by ectopic expression of HSP90. The results from coimmunoprecipitation assays also indicated that HSP90 interacts directly with SP1 protein in *Cdkn1b*$^{+/+}$ cells (Figure 6(h)). Collectively, our results provide clear, direct evidence revealing that upregulated HSP90 is responsible for CDKN1B promotion of SP1 protein stability.

Discussion

Although initially recognized as an inhibitor of cyclin E-CDK2 complexes, CDKN1B is also known to perform cyclin and CDK-independent functions such as, mediation of apoptosis, cytoskeleton rearrangements, and transcriptional regulation [27]. In the present study, we investigated the role of CDKN1B as an atypical tumor suppressor in regulating another key tumor suppressor, PHLPP1, which has never been explored before. Our results indicate that CDKN1B-regulated HSP90 could stabilize the SP1 protein, which initiates *Sqstm1* transcription and expression, in turn promoting autophagy-mediated degradation of *Mir6981*, further reducing its binding to 5′-UTR of *Phlpp1* mRNA, and consequently increasing PHLPP1 protein translation. These novel findings provide new insight into the crosstalk between the 2 tumor suppressors, CDKN1B and PHLPP1 in modulation of normal cell function as schematic illustration in Figure 6(i).

PHLPP1 is known to be a tumor suppressor involved in regulation of various cellular functions. Although our recent studies show that PHLPP1 expression is regulated at the translational level by *Mir190* in an NFKB1-dependent manner [28], its regulation remains largely unknown. In the current studies, we show that PHLPP1 is regulated by CDKN1B at the translational level through the newly identified *Mir6981*. Furthermore, we have discovered that the inhibition of PHLPP1 translation by *Mir6981* is through its specific binding to the 5′-UTR region of *Phlpp1* mRNA, which is distinctly different from the mechanism where most miRNA binds to the 3′- UTR of its targeted mRNA and affects mRNA stability and protein translation. Though the detailed mechanism between the mRNA 5′-UTR and *Mir6981* action is still unknown, the alteration of mRNA's secondary structure following the interaction of the 5′-UTR with miRNA [11,29] might be anticipated as an explanation for *Mir6981*-mediated PHLPP1 protein translation.

Mir6981 is a newly identified miRNA with unknown function, that has been reported in a study in mouse tissues [30]. Our current studies are not only the first to identify *Mir6981* expression in MEF cell lines, we are also the first to show their function as directly binding to the 5′-UTR of *Phlpp1* mRNA, which attenuates tumor suppressor PHLPP1 protein translation, revealing a potential oncogenic function of *Mir6981* in intact cells. The posttranscriptional regulation of mature miRNA has been barely elucidated in previous studies. To the best of our knowledge, there is only a 2014 report by Shenghui Lan *et. al.*, which indicates that autophagy mediates the degradation of *Mir224* in hepatocellular carcinoma [14]. In our current study, we have discovered that autophagy selectively degrades *Mir6981*, and that this degradation can be negatively regulated by CDKN1B. The inhibition of autophagy using the autophagy chemical inhibitor BAF significantly reverses *Mir6981* expression. Moreover, our experiments show that *Mir6981* is recruited to the autophagosome by virtue of its binding with the autophagy receptor SQSTM1, which is recognized by LC3. Therefore, the autophagy receptor SQSTM1 binds directly to *Mir6981* and promotes the autophagy-dependent *Mir6981* degradation initiated by CDKN1B in the intact cells.

It is well known that autophagy mediates SQSTM1 protein degradation, while the regulatory effects of SQSTM1 on autophagy are still controversial based on experimental systems [18]. SQSTM1 has been reported to promote MTORC1 activation, which negatively acts on initiation of autophagy in NIH-3T3 cells *via* modulation of MTORC1 translocation to the lysosomal surface [31], suggesting an inhibitory effect on autophagy [32], whereas in HEK293 and HeLa cells, SQSTM1 is able to liberate BECN1 by disrupting the association between BECN1 and BCL2, revealing that SQSTM1 positively induces autophagy [33]. Our current studies show that ectopic expression of SQSTM1 promotes autophagy in cells accompanied by the induction of BECN1 in *Cdkn1b*-deficient cells, revealing that BECN1 is a SQSTM1 downstream effector, responsible for the increased autophagic activity and degradation of SQSTM1-*Mir6981* complex in *Cdkn1b*-deficient cells. Our results show the regulatory function of CDKN1B in the promotion of SQSTM1 expression and autophagy provides significant insight into understanding the nature of CDKN1B contribution to SQSTM1-induced cell autophagy in the intact cells.

SQSTM1 protein expression is regulated at multiple levels, including protein degradation and mRNA transcription [34,35]. Autophagy defects lead to accumulation of SQSTM1 protein [36]. Multiple transcription factors enhance tumor growth in some cancer tissues by upregulating SQSTM1 transcription, whereas SP1 has been reported to be a regulator of SQSTM1 promoter activity following H_2O_2 treatment in HEK293 cells [37]. Our recent studies indicate that environmental nickel exposure upregulates SQSTM1 protein expression through induction of mRNA and protein in human bronchial epithelial cells [38]. The exploration of the mechanisms underlying nickel regulation of *SQSTM1* mRNA show that nickel upregulates *SQSTM1* mRNA due to transcriptional activation of the *SQSTM1* promoter *via* the *NFKB*-dependent cascade [38]. By tracking the upstream pathway involved in SQSTM1 alteration upon *Cdkn1b* deletion, our current studies show that CDKN1B can activate *Sqstm1* transcription through an SP1-dependent manner, as supported by various deletions of *Sqstm1* promoter-driven luciferase reporters and anti-SP1 antibody affinity-isolation ChIP assay that show SP1 binding to the SP1 binding site in the *Sqstm1* promoter region. Our studies also provide evidence that HSP90 acts as a CDKN1B downstream mediator to stabilize SP1 protein *via* prevention of SP1 proteasome-dependent protein degradation in mouse normal MEFs and mouse epidermal Cl41 cells. Our most recent studies show that in human invasive bladder cancer cells, CDKN1B inhibits CAPN1 proteolysis cascade through attenuation of the JAK1 (Janus kinase 1)-STAT1 (signal transducer and activator of transcription 1) axis to stabilize HSP90 protein, which directly binds to PHLPP2 protein and protect

it from degradation [23]. The elevated PHLPP2 promotes *SQSTM1* transcription and in turn mediates autophagy to enhance MMP2 (matrix metallopeptidase 2) protein degradation, therefore exhibits an inhibition of bladder cancer cell invasion [23]. These results reveal that CDKN1B is able to promote *Sqstm1* transcription and SQSTM1-mediated autophagy through elevating HSP90 expression in both normal MEFs and bladder cancer cells; however, the mechanisms underlying upregulation of *Sqstm1* transcription by CDKN1B-HSP90 are different. Transcription factor SP1, but not JUN, acts as a direct downstream of HSP90 responsible for initiating transcription of *Sqstm1* in normal MEFs (Figure 6), whereas HSP90 directly stabilizes PHLPP2 protein, and consequently activated JUN, but not SP1, leading to *SQSTM1* transcription in human bladder cancer cells [39]. The differential mechanisms of CDKN1B-HSP90 axis in modulation of *Sqstm1* transcription might be due to the differences between mouse normal cells and human cancer cells. It is noted that our current discovery of CDKN1B upregulation of HSP90 is distinctly different from our previous findings showing that CDKN1B exhibits a strong inhibitory effect on HSPB1/HSP27 (heat shock protein family B [small] member 1) and HSPA/HSP70 (heat shock protein family A [Hsp70]) expression at the transcriptional level through MAPK9-JUN- and MAPK9-HSF1-dependent pathways in cell response to arsenite exposure in the same cell lines [27]. Further elucidation of the mechanisms underlying CDKN1B promotion of HSP90 and attenuation of HSPB1 and HSPA will enable us to have a better understanding of the nature of CDKN1B in the regulation of biologic behaviors in the intact cells.

In summary, our studies define an inhibitory effect of CDKN1B on *Mir6981* expression by promoting SQSTM1-dependent autophagic degradation of *Mir6981*. This results in a reduction of the direct binding of *Mir6981* to the 5′-UTR region of *Phlpp1* mRNA, thereby leading to increased PHLPP1 protein translation. Our studies also show that CDKN1B mediates SQSTM1 protein induction through HSP90 stabilization of SP1 protein, which in turn binds to the *Sqstm1* promoter SP1 binding site to initiate *Sqstm1* transcription. Our current studies include the following discoveries: 1) SQSTM1 is a CDKN1B downstream effector and is responsible for CDKN1B-mediated autophagy; 2) by promoting autophagy-mediated degradation of *Mir6981*, CDKN1B exerts a positive regulatory effect on PHLPP1 protein translation; 3) *Mir6981* suppresses PHLPP1 protein translation by binding directly to its mRNA 5′-UTR, rather than to the classical 3′-UTR of mRNA. These novel findings provide significant insight into understanding the crosstalk between 2 tumor suppressors, CDKN1B and PHLPP1, in the regulation of cell function.

Materials and methods

Reagents, antibodies and plasmids

Actinomycin D (sc-200906), CHX (sc-3508), MG132 (sc-201270), and bafilomycin A_1 (BAF) (sc-201550) were purchased from Santa Cruz Biotechnology. Calpain inhibitor was bought from Cayman Chemical (14283). The Dual Luciferase Assay kit was purchased from Promega (E1960). TRIzol (15596026) reagent and SuperScript™ First-Strand Synthesis system (18080,51) were bought from Invitrogen. Antibodies specific against p-MTOR Ser2448, MTOR (9964S), LC3B, ATG3, ATG12–ATG5, ATG7, BECN1 (4445S, autophagy kit), SQSTM1 (88588), ELK1 (9182), GAPDH (5174), p-JUN Ser63 (2361), p-JUN Ser73 (9164), JUN (9165) and TAM67 (5000), were purchased from Cell Signaling Technology. Antibodies specific for CDKN1B (sc-528), JUNB (sc-73), SP1 (sc-14027), E2F1 (sc-193), ACTB (sc-58673) and TUBA (sc-53646) were from Santa Cruz Biotechnology. Specific antibody against PHLPP1 was bought from Bethyl Laboratories (A300661). The shRNAs that specifically target mouse *Cdkn1b* (RMM3981-97059450), *Sp1* (RHS4430-200231665), and their nonsense control (RMM4534) were purchased from Open Biosystems (GE, Pittsburg, PA, USA). The mmu-*Mir6981* expression plasmid (MmiR3993-MR03) and mmu-*Mir6981* inhibitor plasmid (LPP-MMirAN4060-AM04p-100) was bought from GeneCopoeia. The plasmid GFP-*Cdkn1b* was described in our Previous Studies [5]. The plasmid GFP-*Sqstm1* was a gift from Dr. Sung Ouk Kim (University of Western Ontario, London, Ontario, Canada). The plasmid for dominant negative JUN (TAM67) was described in our previous studies [27]. The plasmid containing luciferase reporter under control of mouse *Sqstm1* gene promoter was kindly given by Dr. Alain Bruhat (University of Auvergne, France). The plasmid containing luciferase reporter under control of mouse WT *Phlpp1* mRNA 3′UTR was constructed into pMIRreport vector using the primers: forward 5′-CCC AAG CTT CCC AGC CTG AGT ACT GTT TTA -3′, reverse 5′- GGC AAG CTT TTA CGA CAT GTC CAT TTG G -3′. The plasmid containing luciferase reporter under control of mouse WT *Phlpp1* mRNA 5′UTR was constructed into PGL3-Control vector using the primers: forward 5′- CCC AAG CTT AGC GGC CGC GCC GAA CGC CA -3′, reverse 5′- GGC AAG CTT CGT AGC GGG GCT TCA CGT CG -3′. The primers for cloning the mutant of *Phlpp1* mRNA 5′UTR luciferase reporter are: forward 5′- CCA TCG GCG TCT CCG AAG AGT TCG CGC CGCCGC CG -3′, reverse 5′- CGG CGGCGG CGC GAA CTC TTC GGA GAC GCC GAT GG -3′. The constructed *Phlpp1* mRNA 5′-UTR/3′-UTR luciferase reporter which contains both 5′-UTR and 3′-UTR regulatory regions was constructed using the *Phlpp1* mRNA 3′UTR luciferase reporter *via* the primers: forward 5′- CGC GGA TCC TGG AGC GGC CGC G -3′, reverse 5′- CGC GGA TCC CGT AGC GGG GCT TCA CG -3′. The *Sqstm1* promoter-driven luciferase reporter with mutation of the *Sp1* binding site was constructed using the primers: forward 5′- CAG TGG GGT CGT CTC GAA CCC GTA CCT TTC AAG -3′, reverse 5′- CTT GAA AGG TAC GGG TTC GAG ACG ACC CCA CTG -3′.

Cell lines and transfection

The 3T3 protocol-immortalized mouse embryonic fibroblasts (MEFs), wild-type *Cdkn1b* (*Cdkn1b*$^{+/+}$) and *Cdkn1b*-deficient (*cdkn1b(Δ51)*), were established, as described in our previous studies [5] and cultured in DMEM with 10% FBS. Normal mouse epidermal Cl41 cells were cultured in MEM with 5% FBS [40,41]. Cell transfections were performed with PolyJet™ DNA *in Vitro* Transfection Reagent (SignaGen Laboratories,

SL100468), according to the manufacturer's instructions. For stable transfection, MEF cells were subjected to selection with hygromycin B (200 μg/mL) or puromycin (2.0 μg/mL) depending on the different antibiotic resistance of plasmids transfected. The cells surviving following the antibiotic selection were pooled as mass stable transfectants. Cl41(sh*Cdkn1b*) and Cl41(Nonsense) transfectants were selected by puromycin at 8.0 μg/mL (Alexis, BML-A260-0050).

Cell proliferation assay

Confluent monolayers of cells were trypsinized, and 1×10^3 viable cells suspended in 100 μl of medium were added to each well of 96-well plates. After adherence, cell synchronization was accomplished by replacing culture medium with 0.1% FBS medium for 24 h. Following this, the cells were cultured with 10% FBS medium for the indicated times. The proliferation of the cells was determined using the CellTiter-Glo luminescent cell viability assay kit (Promega, G7570) with a luminometer (Wallac 1420 Victor2 multipliable counter system, Madison, WI, USA).

Flow cytometry assay

The cell cycle distributions were determined by flow cytometry. The cells were cultured in 6-well plates until they were 60% confluent. The cell culture medium was replaced with 0.1% FBS medium for 24 h for cell synchronization, then replaced by 10% FBS medium for another 24 h. Following this, the cells were collected with ice-cold PBS and fixed with 5 ml of 75% ethanol at −20°C overnight. The fixed cells were stained in a buffer containing 0.1% Triton X-100 (Sigma, 9002-93-1), 0.2 mg/ml RNase A (Cell Signaling Technology, 9004S), and 50 μg/ml propidium iodide, then subjected to an EpicsXL flow cytometer (Beckman Coulter Inc., Miami, FL) for cell cycle analysis. The results were analyzed by histogram analysis software (Expo32 v. 1.2).

Western blot analysis

Whole cell extracts were prepared with the cell lysis buffer (10 mM Tris-HCl, pH 7.4, 1% SDS, 1 mM Na_3VO_4) [5] (Thermo Fisher Scientific, Inc. BP16650; Roche, 04693116001) with cocktail (Roche, 04693132001) added. Protein extracts were subjected to western blots with the primary antibodies indicated and probed with the AP-conjugated secondary antibody together with the enhanced chemifluorescence system, as described in a previous report [42]. The images were acquired by scanning with the Typhoon FLA 7000 laser scanner (GE, Pittsburg, PA). Some of the images were calculated by software ImageJ developed by NIH for statistical analysis.

Luciferase reporter assay

Phlpp1 mRNA 3′-UTR luciferase reporter, *Phlpp1* mRNA 5′-UTR luciferase reporter, the *Phlpp1* mRNA 5′-UTR/3′-UTR luciferase reporter and pRL-TK were transfected into *Cdkn1b*$^{+/+}$, *cdkn1b(Δ51)*, and the related transfectants. Twenty-four h after transfection, luciferase activity was determined using the Dual Luciferase Assay system kit, as described in our previous studies [43]. The results were normalized by internal TK signal. The results are expressed as mean ± SD error from 3 independent experiments.

ChIP assay

The EZ-ChIP kit was used to carry out the ChIP assay according to the manufacturer's instructions (Millipore Technologies, 17–371) [44]. Briefly, *Cdkn1b*$^{+/+}$ cells were treated with 1% formaldehyde for 10 min at room temperature. Cells were then resuspended in lysis buffer and sonicated to generate 200 to 400 bp chromatin DNA fragments. After centrifugation (13,000 g for 10 min at 4°C), a 10-fold dilution of the supernatants was incubated with either an anti-SP1 antibody or the control rabbit IgG at 4°C overnight. The immune complex was captured with protein G–agarose beads (Millipore Technologies, 17–371) saturated with salmon sperm DNA (Millipore Technologies, 17–371), and then eluted with elution buffer. The reverse cross-linking of protein-DNA complexes to free DNA was conducted by incubating at 65°C overnight. The DNA was extracted and subjected to PCR analysis. To specifically amplify the region containing the SP1-binding sites in the human *Sqstm1* promoter, PCR was performed with the following pair of primers: 5′- GTC TCG ACC CCG TAC CTT TCA -3′, and 5′- GTC TAG GTA CGG ACG AAA CA -3′. PCR products were separated on 2% agarose gels and stained with ethidium bromide. The images were scanned under UV light, as previously described [42].

RT-PCR

Total RNA was extracted using the TRIzol reagent as described in the manufacturer's instructions and our previous studies [43]. Five μg of total RNA was used for first-strand cDNA synthesis with oligdT primer by SuperScript^{TM}IV First-Strand Synthesis System, as described in our previous studies [42]. Specific primers (Invitrogen) used for PCR amplification were: *mouse Phlpp1*, forward 5′-ACA CCG TGA TTG CTC ACT CC −3′, reverse 5′-TTC CAG TCA GGT CTA GCT CC-3′; *mouse Arap3*, forward 5′-CCC TAC TGT TTG CAC CTA GTG TGT T-3′, reverse 5′-GCC TGG TCC GAG TCA ATA TCA A-3′; *mouse Sqstm1*, forward 5′-GAG AGT GTG GCA GCT GCC CT-3′, reverse 5′-GGC AGC TTC CTT CAG CCC TG-3′; *mouse Sp1*, forward 5′-ATT AAC CTC AGT GCA TTG GGT A-3′, reverse 5′-AGG GCA GGC AAA TTT CTT CTC-3′; and *mouse Actb*, forward 5′-GAC GAT ATT GCC GCA CT-3′, reverse 5′-GAT ACC ACG CTT GCT CTG AG-3′.

Quantitative RT-PCR

The cells were extracted for total RNA using an miRNeasy Mini Kit (QIAGEN, 217,004). One μg of total RNA was used for reverse transcription. Analysis of *Mir7a, Mir103a, Mir135a, Mir196a, Mir199a, Mir503*, and *Mir6981* expression were carried out using the miScript PCR system (QIAGEN,, 218073) by 7900HT Fast Real-time PCR system (Applied

Biosystems, Waltham, MA, USA). The primers for real time PCR assay and internal control *Rnu6* were purchased from Invitrogen. The initial activation was performed at 95°C for 15 min, followed by 40 cycles (denaturation at 95°C for 15 s, annealing at 55°C for 30 s and extension at 72°C for 30 s). The data were analyzed, as described in a previous publication [45].

RNA-IP assay

Cdkn1b$^{+/+}$ cells were cultured in 10-cm dishes. When cell density reached 70 ~ 80%, the cells were extracted using the polysome lysis buffer [10 mM HEPES pH 7 (Sigma, H3375), 100 mM KCl (Mallinckrodt, 8648), 5 mM $MgCl_2$ (EMD Bioscience, MX0045-1), 25 mM EDTA (EM science, 4005), 0.5% NP40 (Sigma, I-30201), 1 mM DTT (Fermentas, RO861), 100 units/ml RNAse OUT (Invitrogen, 10777-019), and complete proteinase inhibitor (Roche, 11697498001)]. The cell lysates were centrifuged at 14,000 × g for 10 min at 4°C. The anti-*Sqstm1* antibody or IgG control (Cell Signaling Technology, 9004S) and A/G agarose beads (Cell Signaling Technology, 9004S) were added into the supernatant and rotated overnight at 4°C in NET2 buffer (50 mM Tris–HCl, pH 7.4, 150 mM sodium chloride, 1 mM magnesium chloride, 0.05% NP40). The beads were washed 3 times and resuspended in 100 µL NET2 and 100 µL SDS-TE (20 mM Tris-HCl, pH 7.5, 2 mM EDTA, 2% sodium dodecyl sulfate), then incubated at 55°C for 30 min, mixing occasionally. The total RNAs in the buffer of the beads were extracted by Trizol (Invitrogen, 15596-026) and real time-PCR was performed to identify the *Mir6981* presented in the immune-complex.

Immunoprecipitation assay

The cells were cultured in 10-cm dishes until the cell concentration reached 70% to 80%. Culture medium was replaced by DMEM containing 0.1% FBS for 12 h. Cells were collected and lysed in 1 × Cell Lysis Buffer (Cell Signaling Technology, 9803) containing protease inhibitors (Roche, 04693132001) followed by brief sonication. Cell extracts were incubated with anti-Hsp90 or anti-mouse IgG (Cell Signaling Technology, 4875) with protein A/G agarose beads overnight at 4°C. Following a brief centrifuge, the beads were washed 3 times with 1 × Cell Lysis Buffer, and the bound proteins were eluted by 2 × SDS sample buffer (Cell Signaling Technology, 7722), then subjected to western blots.

[^{35}S] methionine newly synthesized protein-labeling assays

Cdkn1b$^{+/+}$ and *cdkn1b*(Δ51) cells were incubated with methionine–cysteine-free DMEM (Gibco-BRL, 21013024) containing 2% dialyzed fetal calf serum (Gibco-BRL, 10437036) in the presence of MG132 (50 µM) for 1 h. The cells were then incubated with 2% fetal bovine serum methionine–cysteine-free DMEM containing ^{35}S-labeled methionine/cysteine (250 µCi per dish, ^{35}S-label; Perkin Elmer, NEG009A001MC) for the time periods indicated. The cells were extracted with lysis buffer (Cell Signaling Technology, 9803) containing a complete protein inhibitor mixture and placed on ice for 10 min. Total lysate of 500 mg was incubated with anti-PHLPP1 antibody-conjugated agarose beads at 4°C overnight. The immunoprecipitated samples were washed with the cell lysis buffer 5 times, heated at 100°C for 5 min, and then subjected to sodium dodecyl sulfate–polyacrylamide gel electrophoresis analysis. The ^{35}S-labeled PHLPP1 protein was imaged with the Typhoon FLA 7000 laser scanner.

Statistical analysis

The Student t test was used to determine the significance between treated and untreated groups and the LSD method was used to evaluate the significance among multiple groups. The results are expressed as mean±SD from at least 3 independent experiments. $P < 0.05$ was considered to be a significant difference between the compared groups.

Acknowledgments

We would like to thank Dr. Alain Bruhat from University of Auvergne, France, for providing us with mouse *Sqstm1* promoter-driven luciferase reporter, as well as Dr. James Roberts from Fred Hutchinson Cancer Research Center, Seattle, Washington 98104, USA, for the generous gifts of *cdkn1b*$^{-/-}$ MEF cells. We also thank Ms. Nedda Tichi for her critical reading of the manuscript. This work was partially supported by the grants of NIH/NCI CA165980, CA177665, CA217923 and CA229234, and NIH/NIEHS ES000260.

Disclosure statement

No potential conflict of interest was reported by the authors.

Funding

This work was supported by the NIH/NCI [CA165980];NIH/NIEHS [ES000260]; NIH/NCI [CA229234]; NIH/NCI [CA217923]; NIH/NCI [CA177665].

References

[1] Brognard J, Newton AC. PHLiPPing the switch on AKT and protein kinase C signaling. Trends Endocrinol Metab. 2008 Aug;19(6):223–230.PubMed PMID: 18511290; PubMed Central PMCID: PMCPMC2963565.

[2] Zhou C, Huang C, Wang J, et al. LncRNA MEG3 downregulation mediated by DNMT3b contributes to nickel malignant transformation of human bronchial epithelial cells via modulating PHLPP1 transcription and HIF-1alpha translation. Oncogene. 2017 Jul 06;36(27):3878–3889. PubMed PMID: 28263966; PubMed Central PMCID: PMC5525547.

[3] Wander SA, Zhao D, Slingerland JM. p27: a barometer of signaling deregulation and potential predictor of response to targeted therapies. Clin Cancer Res. 2011 Jan 1;17(1):12–18. PubMed PMID: 20966355; PubMed Central PMCID: PMCPMC3017239.

[4] Sanseverino F, D'Andrilli G, Petraglia F, et al. Molecular pathology of ovarian cancer. Anal Quant Cytol Histol. 2005 Jun;27(3):121–124. PubMed PMID: 16121632.

[5] Zhang D, Liu J, Mi X, et al. The N-terminal region of p27 inhibits HIF-1alpha protein translation in ribosomal protein S6-dependent manner by regulating PHLPP-Ras-ERK-p90RSK axis. Cell Death Dis. 2014;5:e1535. PubMed PMID: 25412313; PubMed Central PMCID: PMCPMC4260754.

[6] Pillai RS, Bhattacharyya SN, Filipowicz W. Repression of protein synthesis by miRNAs: how many mechanisms? Trends Cell Biol. 2007 Mar;17(3):118–126. PubMed PMID: 17197185.
[7] Meister G. Argonaute proteins: functional insights and emerging roles. Nat Rev Genet. 2013 Jul;14(7):447–459.PubMed PMID: 23732335.
[8] Winter J, Jung S, Keller S, et al. Many roads to maturity: microRNA biogenesis pathways and their regulation. Nat Cell Biol. 2009 Mar;11(3):228–234. PubMed PMID: 19255566.
[9] Shen J, Hung MC. Signaling-mediated regulation of microRNA processing. Cancer Res. 2015 Mar 1;75(5):783–791. PubMed PMID: 25660948; PubMed Central PMCID: PMCPMC4348149.
[10] Bartel DP. MicroRNAs: target recognition and regulatory functions. Cell. 2009 Jan 23;136(2):215–233. PubMed PMID: 19167326; PubMed Central PMCID: PMCPMC3794896.
[11] Meijer HA, Kong YW, Lu WT, et al. Translational repression and eIF4A2 activity are critical for microRNA-mediated gene regulation. Science. 2013 Apr 5;340(6128):82–85. PubMed PMID: 23559250.
[12] Pickering BM, Willis AE. The implications of structured 5′ untranslated regions on translation and disease. Semin Cell Dev Biol. 2005 Feb;16(1):39–47.PubMed PMID: 15659338.
[13] Mizushima N, Levine B, Cuervo AM, et al. Autophagy fights disease through cellular self-digestion. Nature. 2008 Feb 28;451 (7182):1069–1075. PubMed PMID: 18305538; PubMed Central PMCID: PMCPMC2670399.
[14] Lan SH, Wu SY, Zuchini R, et al. Autophagy-preferential degradation of MIR224 participates in hepatocellular carcinoma tumorigenesis. Autophagy. 2014 Sep;10(9):1687–1689. PubMed PMID: 25068270; PubMed Central PMCID: PMCPMC4206546.
[15] Duran A, Serrano M, Leitges M, et al. The atypical PKC-interacting protein p62 is an important mediator of RANK-activated osteoclastogenesis. Dev Cell. 2004 Feb;6 (2):303–309. PubMed PMID: 14960283.
[16] Rodriguez A, Duran A, Selloum M, et al. Mature-onset obesity and insulin resistance in mice deficient in the signaling adapter p62. Cell Metab. 2006 Mar;3(3):211–222. PubMed PMID: 16517408.
[17] Sugimoto R, Warabi E, Katayanagi S, et al. Enhanced neointimal hyperplasia and carotid artery remodelling in sequestosome 1 deficient mice. J Cell Mol Med. 2010 Jun;14(6B):1546–1554. PubMed PMID: 19780870.
[18] Lippai M, Low P. The role of the selective adaptor p62 and ubiquitin-like proteins in autophagy. Biomed Res Int. 2014;2014:832704. PubMed PMID: 25013806; PubMed Central PMCID: PMCPMC4075091.
[19] Ichimura Y, Kumanomidou T, Sou YS, et al. Structural basis for sorting mechanism of p62 in selective autophagy. J Biol Chem. 2008 Aug 15;283(33):22847–22857. PubMed PMID: 18524774.
[20] Moscat J, Diaz-Meco MT. p62 at the crossroads of autophagy, apoptosis, and cancer. Cell. 2009 Jun 12;137(6):1001–1004. PubMed PMID: 19524504; PubMed Central PMCID: PMCPMC3971861.
[21] Chu IM, Hengst L, Slingerland JM. The Cdk inhibitor p27 in human cancer: prognostic potential and relevance to anticancer therapy. Nat Rev Cancer. 2008 Apr;8(4):253–267.PubMed PMID: 18354415.
[22] Kiyokawa H, Kineman RD, Manova-Todorova KO, et al. Enhanced growth of mice lacking the cyclin-dependent kinase inhibitor function of p27(Kip1). Cell. 1996 May 31;85 (5):721–732. PubMed PMID: 8646780.
[23] Fero ML, Rivkin M, Tasch M, et al. A syndrome of multiorgan hyperplasia with features of gigantism, tumorigenesis, and female sterility in p27(Kip1)-deficient mice. Cell. 1996 May 31;85 (5):733–744. PubMed PMID: 8646781.
[24] Ruvinsky I, Meyuhas O. Ribosomal protein S6 phosphorylation: from protein synthesis to cell size. Trends Biochem Sci. 2006 Jun;31(6):342–348. PubMed PMID: 16679021.
[25] Schmid DI, Schwertz H, Jiang H, et al. Translational control of JunB, an AP-1 transcription factor, in activated human endothelial cells. J Cell Biochem. 2013 Jul;114(7):1519–1528. PubMed PMID: 23297064; PubMed Central PMCID: PMC3999827.
[26] Wang SA, Chuang JY, Yeh SH, et al. Heat shock protein 90 is important for Sp1 stability during mitosis. J Mol Biol. 2009 Apr 17;387(5):1106–1119. PubMed PMID: 19245816.
[27] Liu J, Zhang D, Mi X, et al. p27 suppresses arsenite-induced Hsp27/Hsp70 expression through inhibiting JNK2/c-Jun- and HSF-1-dependent pathways. J Biol Chem. 2010 Aug 20;285 (34):26058–26065. PubMed PMID: 20566634; PubMed Central PMCID: PMCPMC2924005.
[28] Yu Y, Zhang D, Huang H, et al. NF-kappaB1 p50 promotes p53 protein translation through miR-190 downregulation of PHLPP1. Oncogene. 2014 Feb 20;33(8):996–1005. PubMed PMID: 23396362; PubMed Central PMCID: PMCPMC3883870.
[29] Gu W, Xu Y, Xie X, et al. The role of RNA structure at 5′ untranslated region in microRNA-mediated gene regulation. Rna. 2014 Sep;20(9):1369–1375. PubMed PMID: 25002673; PubMed Central PMCID: PMCPMC4138320.
[30] Ladewig E, Okamura K, Flynt AS, et al. Discovery of hundreds of mirtrons in mouse and human small RNA data. Genome Res. 2012 Sep;22(9):1634–1645. PubMed PMID: 22955976; PubMed Central PMCID: PMCPMC3431481.
[31] Moscat J, Diaz-Meco MT. Feedback on fat: p62-mTORC1-autophagy connections. Cell. 2011 Nov 11;147(4):724–727. PubMed PMID: 22078874; PubMed Central PMCID: PMCPMC3290994.
[32] Duran A, Amanchy R, Linares JF, et al. p62 is a key regulator of nutrient sensing in the mTORC1 pathway. Mol Cell. 2011 Oct 7;44(1):134–146. PubMed PMID: 21981924; PubMed Central PMCID: PMCPMC3190169.
[33] Zhou L, Wang HF, Ren HG, et al. Bcl-2-dependent upregulation of autophagy by sequestosome 1/p62 in vitro. Acta Pharmacol Sin. 2013 May;34(5):651–656. PubMed PMID: 23564079; PubMed Central PMCID: PMCPMC3647217.
[34] Komatsu M, Ichimura Y. Physiological significance of selective degradation of p62 by autophagy. FEBS Lett. 2010 Apr 2;584 (7):1374–1378. PubMed PMID: 20153326.
[35] Vadlamudi RK, Shin J. Genomic structure and promoter analysis of the p62 gene encoding a non-proteasomal multiubiquitin chain binding protein. FEBS Lett. 1998 Sep 18;435(2–3):138–142. PubMed PMID: 9762895.
[36] Mathew R, Karp CM, Beaudoin B, et al. Autophagy suppresses tumorigenesis through elimination of p62. Cell. 2009 Jun 12;137 (6):1062–1075. PubMed PMID: 19524509.
[37] Du Y, Wooten MC, Wooten MW. Oxidative damage to the promoter region of SQSTM1/p62 is common to neurodegenerative disease. Neurobiol Dis. 2009 Aug;35(2):302–310. PubMed PMID: 19481605.
[38] Huang H, Zhu J, Li Y, et al. Upregulation of SQSTM1/p62 contributes to nickel-induced malignant transformation of human bronchial epithelial cells. Autophagy. 2016 Oct 02;12 (10):1687–1703. PubMed PMID: 27467530; PubMed Central PMCID: PMC5079680.
[39] Peng M, Wang J, Zhang D, et al. PHLPP2 stabilization by p27 mediates its inhibition of bladder cancer invasion by promoting autophagic degradation of MMP2 protein. Oncogene. 2018 June 21. DOI:10.1038/s41388-018-0374-1.
[40] Zhu J, Zhang J, Huang H, et al. Crucial role of c-Jun phosphorylation at Ser63/73 mediated by PHLPP protein degradation in the cheliensisin a inhibition of cell transformation. Cancer Prev Res (Phila). 2014 Dec;7(12):1270–1281. PubMed PMID: 25281487; PubMed Central PMCID: PMCPMC4256147.
[41] Gao G, Chen L, Li J, et al. Isorhapontigenin (ISO) inhibited cell transformation by inducing G0/G1 phase arrest via increasing MKP-1 mRNA Stability. Oncotarget. 2014 May 15;5 (9):2664–2677. PubMed PMID: 24797581; PubMed Central PMCID: PMCPMC4058035.

[42] Jin H, Yu Y, Hu Y, et al. Divergent behaviors and underlying mechanisms of cell migration and invasion in non-metastatic T24 and its metastatic derivative T24T bladder cancer cell lines. Oncotarget. 2015 Jan 1;6(1):522–536. PubMed PMID: 25402510; PubMed Central PMCID: PMCPMC4381612.

[43] Xu J, Wang Y, Hua X, et al. Inhibition of PHLPP2/cyclin D1 protein translation contributes to the tumor suppressive effect of NFkappaB2 (p100). Oncotarget. 2016 Apr 15 PubMed PMID: 27095572.

[44] Fang Y, Cao Z, Hou Q, et al. Cyclin d1 downregulation contributes to anticancer effect of isorhapontigenin on human bladder cancer cells. Mol Cancer Ther. 2013 Aug;12(8):1492–1503. PubMed PMID: 23723126; PubMed Central PMCID: PMCPMC3744103.

[45] Zeng X, Xu Z, Gu J, et al. Induction of miR-137 by isorhapontigenin (ISO) directly targets SP1 protein translation and mediates its anticancer activity both in vitro and in vivo. Mol Cancer Ther. 2016 Mar;15(3):512–522. PubMed PMID: 26832795; PubMed Central PMCID: PMCPMC4783212.